J Mar Sci Technol (2018) 23:580–595
https://doi.org/10.1007/s00773-017-0494-2

ORIGINAL ARTICLE

Permanent set evolution of aluminium-alloy plates due to repeated impulsive pressure loadings induced by slamming

Dac Dung Truong[1] · Hyun Kyoung Shin[1] · Sang-Rai Cho[1]

Received: 12 June 2017 / Accepted: 20 October 2017 / Published online: 1 November 2017

Abstract This study investigates the response of marine aluminium-alloy plates to repeated impulsive pressure loadings due to slamming. The numerical simulations performed using the ABAQUS commercial software package were validated against relevant experimental data from the open literature. In the calculations, linear strain hardening was applied and no strain-rate hardening was considered owing to the insensitivity of the aluminium alloys to strain rate. The triangular pressure pulses with linear decay and isosceles are idealised for water-pressure impact profiles. A fully clamped unstiffened plate made of Al 5083-O with practical plate slenderness ratios is considered. The effect of the typical heat-affected zone is also numerically evaluated. Simple yet accurate closed-form equations for the prediction of the permanent set evolution of the plates due to repeated impulsive pressure loadings are derived based on the parametric study results. The results showed that the permanent set of plates was significantly increased for the first few repeated impulsive pressure loadings, while later, the total permanent set tended to have certain values regardless of the impulsive pressure and aspect ratio. Therefore, this indicates that the effect of the repetition of impulsive pressure loadings cannot be neglected in marine structural designs.

✉ Sang-Rai Cho
srcho@ulsan.ac.kr

Dac Dung Truong
truongdacdung@ntu.edu.vn

Hyun Kyoung Shin
hkshin@ulsan.ac.kr

[1] School of Naval Architecture and Ocean Engineering, University of Ulsan, 93 Daehak-ro, Namgu, Ulsan 44610, South Korea

Keywords Slamming · Aluminium-alloy plate · Permanent set · Repeated pressure impact · Nonlinear FE analysis

1 Introduction

During the last two decades, high-strength aluminium alloys have been widely and increasingly applied to marine structures including high-speed crafts and offshore structures owing to their low weight and non-corrosive properties. In addition, the energy absorption capacity per-unit-density of aluminium is high as compared to conventional steel. To gain a better understanding of the impact problem and develop reliable design tools, it is important to thoroughly understand the material and structural dynamic behaviour of structures under extreme loadings that were built using aluminium alloys.

During their service life, marine structures tend to be subjected to repeated impulsive pressure loads due to slamming, sloshing, and green water. From these, only the repeated impulsive pressure loading due to slamming will be considered in this study. Even in a single storm, ships or offshore structures can be impacted owing to the repeated occurrence of slamming, which leaves permanent sets at the impacted region and the repetition of these slam impact loads over time may then lead to serious damage to the structures. To date, no design guidance regarding the allowable permanent set due to slamming has been published. However, it is necessary to be able to estimate the permanent set for a more deliberate design of marine structures, particularly for high-speed vessels, for withstanding slamming.

Nowadays, high-speed vessel designs strongly rely on semi-empirical design methods provided by classification societies [1–3]. The slamming impulsive pressure is

assumed to be quasi-static neglecting its dynamic nature. The basis of this assumption is the long duration of the impulse as compared to the fundamental period of vibration of the impacted structure [4]. At this point, it may be asked whether the dynamic nature of impulsive pressures can be neglected, thus allowing it to be considered as quasi-static. As stated by Ref. [5], for practical design purposes, the problem of impact pressure actions in terms of structural behaviour can conveniently be idealised within three domains: (1) impulsive domain when $t_d/T_n < 0.3$, (2) dynamic domain when $0.3 < t_d/T_n < 3$, and (3) quasi-static domain when $t_d/T_n > 3$, where t_d is the duration of the impact loading, and T_n is the fundamental period of vibration corresponding to the lowest natural frequency of the structure.

As mentioned earlier, the repetition is a distinctive characteristic of marine impulsive pressure loadings. When vessels are larger and faster, actual slamming-induced repeated impulsive pressure loads caused greater local damage in the vessels structural members. Although the slamming problems considering single load have been extensively studied, only a few studies have investigated the effects of load repetition on the extent of damage on impacted structures [6–9]. Among these few studies, several researchers focused on steel structures. Yuhara [6] performed repeated wet drop tests on two clamped ship bow models made of 9 mm mild steel and found that the equivalent static pressure can be represented by the corresponding repeated impact pressure. Caridis and Stefanou [7] numerically studied the effects of several load impacts on an unstiffened plate. The amplitude of the applied impulsive pressure was 1.5 times that of the static collapse value of the plate. The permanent set was increased by approximately 40% after the fourth impact. Recently, Shin et al. [8] conducted several repeated drop tests on unstiffened plates with various thicknesses for different drop heights. They concluded that the increment in the permanent set cannot be neglected, and a dynamic approach is required to be employed to account for this phenomenon. Furthermore, in the case of structures fabricated from marine aluminium alloys, Mori and Nagai [10] and Mori [9] investigated the response of the bottom plate to slamming by performing single and repeated wet drop tests on full- and small-scale models of the bottom plates of high-speed crafts, respectively. They also provided the theoretical results obtained using the finite strip method, which agreed well with the test results.

With respect to the other types of loadings applied to marine aluminium-alloy panels, there are several published studies on the ultimate strength of aluminium-alloy structures. The available literature includes studies on the structural response of aluminium plates and stiffened panels subjected to monotonically increasing extreme in-plane loads [11–13] as well as methods on predicting the progressive collapse of aluminium hull girders [14]. Thus far, little effort has been focused on the plastic damage to marine aluminium-alloy structures subjected to repeated impulsive pressure loadings induced by slamming in real cases.

In this study, the response of marine aluminium-alloy plates to repeated impulsive pressure loadings induced by slamming was numerically studied. The repeated wet drop tests on stiffened marine aluminium-alloy plates in the available literature were used to validate the present numerical simulations using the ABAQUS commercial software package. Based on a rigorous parametric study, the simple, yet accurate formulae for the prediction of a permanent set of plates due to repeated impulsive pressure loadings are derived using nonlinear regression analysis. The effect of the typical heat-affected zone (HAZ) is also numerically investigated. The results showed that permanent sets of plates are significantly increased for the first few impulsive pressure loadings, while later, the total permanent set tended to have certain values regardless of the impulse and aspect ratio. Therefore, this indicates that the effect of the repetition of the impulsive pressures cannot be neglected in marine structural design against slamming.

2 Brief descriptions of repeated wet drop tests

The repeated wet drop tests conducted by Mori [9] on two stiffened aluminium-alloy plates, representing the bottom of a high-speed craft, were used for substantiation of current numerical analysis models. Two models were manufactured using 6-mm thick 5083-O aluminium alloy. The dimensions of the two stiffened aluminium-alloy plates, along with the points at which the water pressure, strain, and deflection were measured, are shown in Fig. 1. It should be noted that to study the effect of flexibility of the stiffeners on the elastic responses, the cross sections of the stiffeners in the two models were designed with different sizes. Model No. 1 represented the bottom of an actual high-speed craft, while the stiffener rigidity of model No. 2 was half of model No. 1. The mechanical properties of the aluminium-alloy material of the models are summarised in Table 1. The drop test was repeated nineteen times for model No. 1, while changing the drop height from 0.3 to 1.6 m, and it was repeated seven times for model No. 2, while changing the drop height from 0.3 to 1.0 m, as presented in Table 2. To measure the water pressure and strain of the models, two pressure gauges (P1 and P2) and three strain gauges (S1, S2, and S3) were attached to the models, as shown in Fig. 1.

From the pressure histories obtained from the tests, the characteristics of the impulses in terms of peak pressure, and impulse duration were determined and are listed in Table 2. It should be noted that the strain gauge S3 located at the mid-length of the flange was not considered for model No. 2. The permanent set of the models was

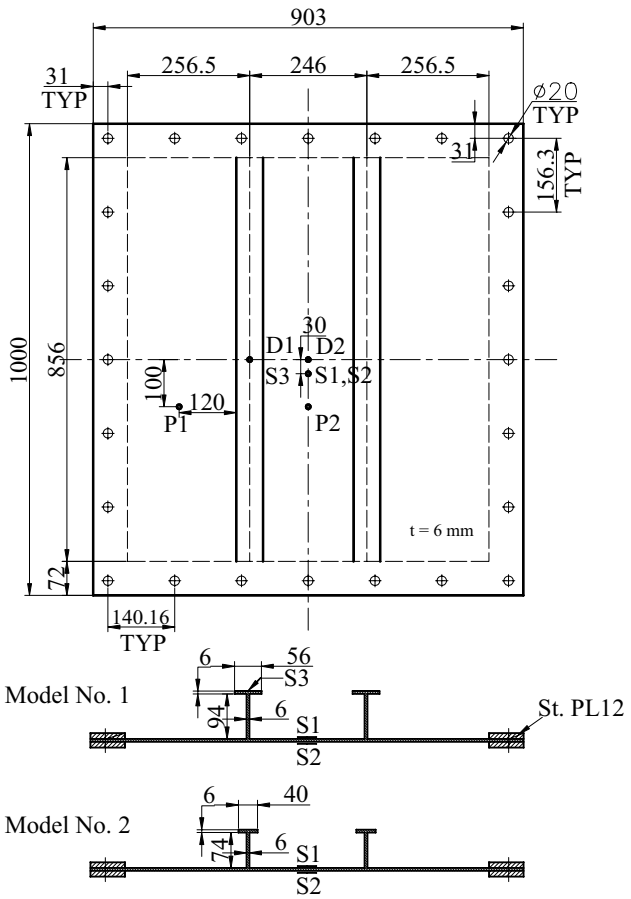

Fig. 1 Geometry of the stiffened aluminium plates (unit: mm) [10]

Table 1 Mechanical properties of test model material [10]

Material	Yield strength, σ_0 (MPa)	Young's modulus, E (MPa)	Hardening modulus, E_h (MPa)	Density, ρ (kg/m^3)	Poisson's ratio, ν
Al 5083-O	134.4	68,700	2750	2700	0.3

recorded during each drop at D1 and D2, at the centre of the stiffener flange and plate, respectively. The water pressures were recorded at P1 and P2. The measured pressures generally increased as the drop height increased. However, the difference in pressures between P1 and P2 decreased when the drop height increased. In addition, the measured pressures decreased slightly at high drop heights, owing to the increase in the number of air layers [9]. The durations of the pressure loads recorded for the various drop heights were almost identical, therefore, in the numerical validation model, the pressure duration will be maintained a constant value for all impulses. Detailed information regarding the experiment can be found in Ref. [9]. The test results are summarised in Table 2, along with the current numerical analysis results.

3 Finite element modelling

The evolution of the permanent set of stiffened aluminium-alloy plates obtained from the repeated wet drop tests conducted by Mori [9] was employed to substantiate the present nonlinear finite element (FE) analysis. Here, the numerical computations were performed using the ABAQUS/Explicit commercial software package. Owing to its symmetry condition, a quarter FE model consisting of the stiffened plate model and support plates, as shown in Fig. 2, was considered to reduce the required computation time.

3.1 Mesh size and contact definition

The stiffened plate model and support plates (see Fig. 2) were meshed with the four-node shell element S4R from the ABAQUS element library. Five integration points were used through the thickness and the default hourglass controls were used for this element. To evaluate the computational efficiency and accuracy, convergence tests were performed for various mesh sizes. Based on the convergence test results the determined mesh sizes of the plate model and support plates were 5×5 mm and 10×10 mm, respectively.

The "surface-to-surface contact" option from the ABAQUS contact library was selected for representing the contact between the plate model and support plates. The penalty and "hard" contact methods were used to define the tangential and normal interaction behaviour of any possible self-contact among the model parts during impacts. After performing a set of preliminary analyses, the friction coefficient between the plate model and support plates was set as 0.2, which is also consistent with the value proposed by Villavicencio and Guedes Soares [15].

3.2 Definition of material properties

To properly represent the material of the test models, the mechanical properties of the material that were provided by Mori [9] were used in the current numerical models. In the analysis, a simple linear hardening expression for a true stress–strain relation, proposed by Park and Cho [16], with an isotropic hardening model, was employed using Eq. 1. It should be noted that, although the kinematic hardening and combined isotropic–kinematic hardening models may be more realistic to describe the constitutive relationship of the material considering the effect of the elastic spring-back on hardening behaviour (including Bauschinger effect) for cyclic loading or load reversals, it is difficult to use this model based on the data

Table 2 Test conditions and comparisons of numerical predictions and test results for the permanent set

Model	Drop height (m)	Number of repetitions	Impact	*Pressure (MPa)	Impact duration (ms)	Permanent set/plate thickness, w_p/t [-]				X_m	
						Exp.		Num.		Num./Exp.	
						D1	D2	D1	D2	D1	D2
No. 1	0.3	1	1	0.121	10.269	0.178	0.418	0.210	0.405	1.18	0.97
	0.4	2	2	0.136		0.213	0.452	0.228	0.429	1.07	0.95
			3	0.216		0.213	0.452	0.245	0.452	1.15	1.00
	0.6	2	4	0.240		0.321	0.679	0.341	0.608	1.06	0.89
			5	0.279		0.333	0.725	0.353	0.623	1.06	0.86
	0.8	3	6	0.302		0.511	0.938	0.519	0.946	1.01	1.01
			7	0.302		0.523	0.962	0.529	0.958	1.01	1.00
			8	0.322		0.593	0.999	0.542	0.976	0.91	0.98
	0.9	2	9	0.341		0.619	1.034	0.639	1.159	1.03	1.12
			10	0.322		0.629	1.106	0.651	1.174	1.03	1.06
	1.0	2	11	0.341		0.641	1.178	0.668	1.205	1.04	1.02
			12	0.358		0.689	1.199	0.732	1.304	1.06	1.09
	1.1	2	13	0.320		0.725	1.319	0.756	1.342	1.04	1.02
			14	0.358		0.760	1.449	0.757	1.343	1.00	0.93
	1.3	2	15	0.333		0.809	1.496	0.757	1.344	0.94	0.90
			16	0.367		0.891	1.663	0.803	1.415	0.90	0.85
	1.5	2	17	0.381		1.033	2.078	0.917	1.570	0.89	0.76
			18	0.396		1.342	2.468	0.962	1.642	0.72	0.67
	1.6	1	19	0.386		1.403	2.789	0.965	1.646	0.69	0.59
No. 2	0.3	2	1	0.135	11.786	0.252	0.464	0.343	0.529	1.36	1.14
			2	0.139		0.294	0.489	0.343	0.530	1.17	1.08
	0.4	2	3	0.148		0.329	0.608	0.352	0.541	1.07	0.89
			4	0.167		0.359	0.608	0.383	0.581	1.07	0.96
	0.6	1	5	0.244		0.543	0.916	0.617	0.919	1.14	1.00
	1.0	2	6	0.260		1.114	1.840	1.090	1.549	0.98	0.84
			7	0.330		1.186	2.430	1.172	1.657	0.99	0.68

* Mean pressure of P1 and P2

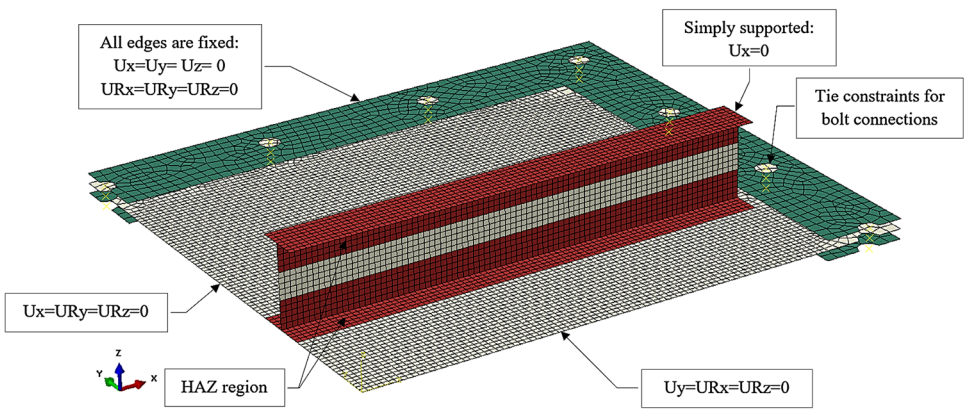

Fig. 2 Quarter FE model of test model

of material properties provided by Mori [9], which are the yield strength and Young's and hardening modulus only. In addition, only monotonic tensile test results were reported and cyclic tensile tests on the current materials were not found in the available literature. Therefore, the isotropic hardening model was applied based on monotonic tensile test results provided in Ref. [9]. The adequacy of applying

this isotropic hardening model for repeated impact simulations was confirmed by other studies [17, 18].

$$\sigma_{tr} = \sigma_0 + \frac{E \times E_h}{E - E_h}\varepsilon_p \quad (1)$$

where σ_{tr} is the true stress corresponding to the equivalent plastic strain ε_p, σ_0 is the yield strength, E is the Young's modulus, and E_h is the hardening modulus, as given in Table 1. The true stress and plastic strain curves applied in the numerical model are shown in Fig. 3.

It is known that owing to the insensitivity of aluminium alloys to the strain rate in the case of dynamic loading from high-velocity impacts [19], the strain rate was not considered in the numerical modelling of the rate-dependent material behaviour of Al 5083-O in this study. A recently conducted experimental study [20] also confirmed this.

3.3 Boundary conditions

The four edges of the support plate were restrained simulating the experimental boundary conditions. To simplify the bolt connections, a tie constraint was applied to model the bolt connections between the plate model and the support plates. However, the ends of the stiffeners were free in all the degrees of freedom with the exception of the translation in the x-direction. The boundary conditions applied in the quarter numerical models are shown in Fig. 2.

3.4 Heat affected zone

Owing to the fusion welding fabrication of the test models, the HAZ should be considered in the numerical simulations. Fusion welding on aluminium plates resulted in the formation of an HAZ. As the heat generated caused the area adjacent to the weld to be slightly annealed, a considerable loss in strength was observed. In this study, the effects of the HAZ on the mechanical properties of the welded areas of aluminium alloys were assumed as a parameter of influence, say "knockdown" factor. The HAZ effect will be included in the numerical modelling of the tested plate models.

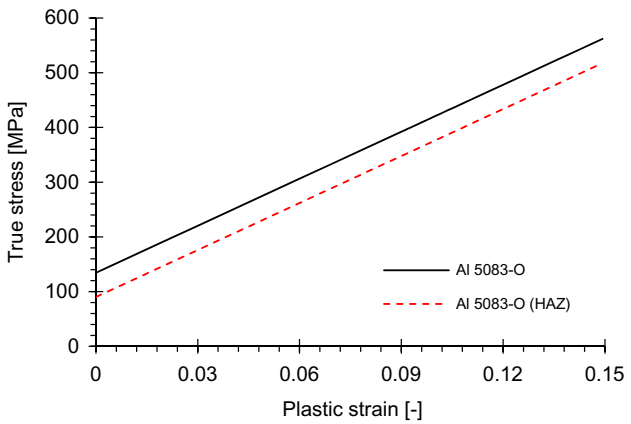

Fig. 3 True stress–plastic strain curves for Al 5083-O base material and HAZ

For the purpose of simplicity, the strength loss is usually assumed to be uniform in the HAZ, and the yield strength in the HAZ can be approximated using a knockdown factor. As in Ref. [21], in this study, a strength knockdown factor of 0.67 was approximated for Al 5083-O. The knockdown factor was applied to both the yield strength and the entire true stress–plastic-strain curve of Al 5083-O, based on the assumption that the strain hardening characteristics of Al 5083-O are maintained in the HAZ. The true stress–plastic-strain curves for the plate with and without HAZ are shown in Fig. 3. Irrespective of the plate dimensions, the width of the HAZ was considered to be 25 mm for this study, based on results from the experiments conducted by Zha and Moan [22] and Paik and Duran [12] and numerical investigations by several other researchers [11, 23–25]. The locations for the HAZ are shown in red in Fig. 2. Furthermore, as residual stresses were generated by the welding, these stresses were necessarily introduced in the numerical plate model. It was assumed that, across the HAZ width of 25 mm, a tensile residual stress is equal to the yield strength of the HAZ material [21, 24, 26], and the corresponding compressive residual stress was then determined by assuming the equilibrium of the internal forces [11].

3.5 Simplification of pressure history and scenario of repeated loadings

The complex slamming pressure histories recorded by Mori [9] (see Fig. 4a) were idealised as triangular pressure pulses with linear rise and decay based on the peak pressure value and peak duration, as shown in Fig. 4b, as proposed by Jones [27], and also confirmed by Cho et al. [28]. It should be noted that as the actual duration of the peak of the impulse induced by slamming was greater than the fundamental period of the impacted plate [9], it is concluded that the effects of the tail part on the extent of damage would be negligible. Here, repeated impulsive pressure loadings are simulated by performing the calculations repeatedly. After each triangular pressure pulse, artificial material damping is introduced in the model using the Rayleigh damping model to overcome elastic vibrations caused by the impulsive pressure, and to quickly approach a static equilibrium state. The Rayleigh damping consists of the mass proportional part associated with low frequency oscillations and stiffness proportional part associated with high frequency oscillations. The former was used by including a damping matrix in the dynamic analysis, which is obtained by multiplying the mass matrix of the system with a coefficient α. It was observed

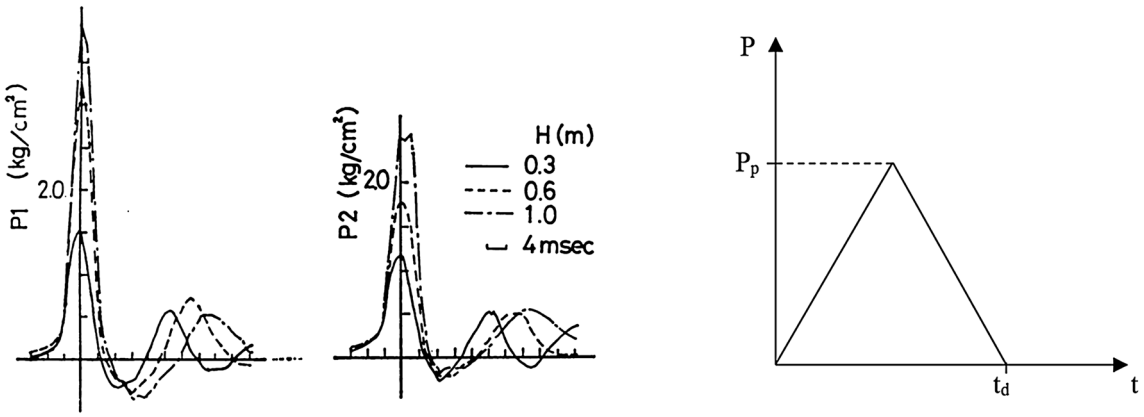

a Recorded data [10] **b** Idealized load profile

Fig. 4 Pressure history applied for validation of numerical simulations

that the damping model reduced permanent set. To obtain an adequate value of α, preliminary analyses were conducted varying the damping coefficients. It showed that when the coefficient α was set as the lowest natural frequency of the model, the permanent set reduced by 5.24 and 3.96% for models Nos. 1 and 2, respectively. Considering the computational efficiency, the lowest natural frequency of the model was employed as the value of coefficient α. The next impulse is then applied to the plate to simulate the subsequent impacts. It should be noted that the impulses were assumed to be uniformly distributed over the entire surface of the stiffened plate. In each of the restarted analyses, the deformed shape, residual stresses, and strain, in the current model, due to the previous impulse, are preserved using multiple steps of ABAQUS/Explicit [29].

3.6 Validation of numerical analysis model

The numerical analysis model is validated by comparing the numerical results with the available slamming test results mentioned in Sect. 2. It should be noted that the simulations of the tests were performed using the measured pressure histories. The permanent sets at the mid-length of the flange of the stiffeners and the centre of the plate, which were denoted as D1 and D2, respectively, were used as the basis for assessing the accuracy of the numerical predictions. The results and the details of the loading in each test are listed in Table 2. The comparison between the evolution of the permanent set obtained numerically and the test results is plotted in Fig. 5. In the figure, 'D1_Exp' and 'D2_Exp.' denoted the experimental permanent set measured at D1 and D2, respectively, while 'D1_Num._Mid-flange point' and 'D2_Num._Center point' denoted the numerically predicted permanent set at D1 and D2, respectively. From Table 2 and Fig. 5, it is evident that the numerical predictions correlate

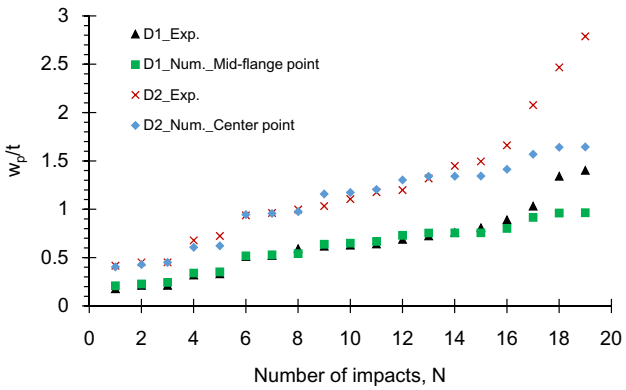

a Model No. 1

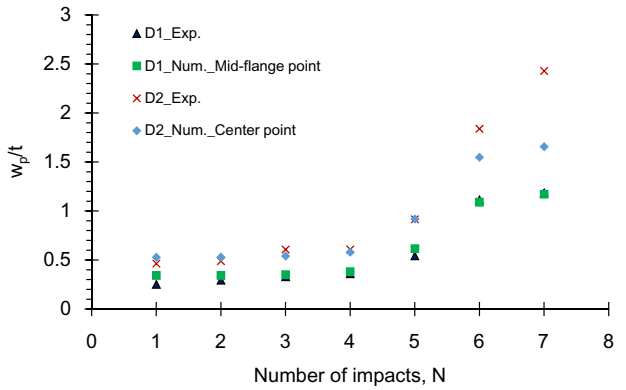

b Model No. 2

Fig. 5 Permanent set of tested models versus number of impacts

well with the experimental results. Except for the first impact at D1, and the last three impacts at D2 of model No. 1, and the first impact at D1 and last two impacts at D2 of model No. 2, the percentage difference between the experimental

and numerical results is less than 10%. The permanent set of the plates obtained both numerically and experimentally increased with the number of impacts, and the increment in the permanent set was reduced for the same applied pressure. However, there are significant discrepancies in the predicted and experimentally obtained values for the last three impacts of model No. 1 at both D1 and D2, and for the last two impacts of model No. 2 at D2. The deflections at those points were abruptly increased. It is premature to mention regarding the sources of the errors unless more experimental information is provided including the thinning of the model plates and occurrence of fracture at boundaries. In general, however, considering the large uncertainties in slamming tests as compared to those of static tests, it can be concluded that the numerical analysis method employed in this study is reasonably accurate and reliable. A parametric study is presented in the next section of this paper.

4 Parametric study

The validated model was employed to perform a rigorous parametric study to examine the effect of the change in impulse in terms of peak pressure and load duration, the profile of the triangular pulse and aspect ratio. The purpose of this work is to empirically derive simple design formulae for estimating the permanent set of plates under slamming, which will be described in detail later. The HAZ, with the assumption described in the previous section, is applied to the four edges of the fully clamped plate, as illustrated in Fig. 6, where the HAZ pattern represents the welding method used for the 5xxx series of the flat plate sheet [21].

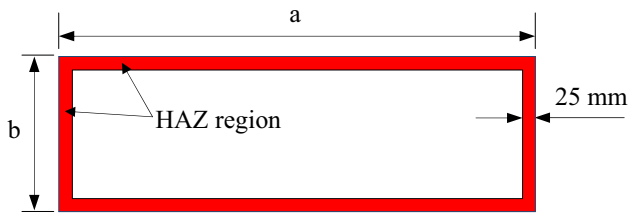

Fig. 6 HAZ location in fully clamped plates applied in the current numerical models

4.1 Plate models and material properties

Based on the full-scale tested model No.1 mentioned in the previous section, the 3, 6, and 7 mm thick plate models with a breadth of 246 mm, were selected as an isolated plate to represent the real unstiffened plate bounded by stiffeners. It should be noted that the plate slenderness ratios, β, in Eq. 2, was varied in the range 1.55–3.63 in this study.

$$\beta = \frac{b}{t}\sqrt{\frac{\sigma_0}{E}} \tag{2}$$

where b is the plate breadth and t is the plate thickness.

The characteristics of the clamped plates are given in Table 3. It should be noted that only rectangular unstiffened plates were considered in this study. To realistically represent materials commonly used to fabricate the marine panels, the material Al 5083-O, the same as that used in Mori's model [9], was considered in the parametric study. Furthermore, the strain-rate effect was neglected in the current simulations.

4.2 Load characteristics

As the mentioned validation simulations, the load was assumed to be uniformly distributed over the entire surface of the plate. It should be noted that the impacts are repeated 10 times with the same impulse in this parametric study.

Table 3 Dimensions and other corresponding parameters calculated using Eqs. 3, 4, 5, 6 for parametric study

Plate #	Aspect ratio, *a/b*	Dimension, $a \times b \times t$ (mm)	Plate slenderness ratio, β	Fundamental period, T_n (ms)	Static collapse pressure, P_c (MPa)	P_p/P_c	T_d/T_n
1	2	492 × 246 × 3	3.63	3.303	0.141	1.5, 2.0, 3.0, 4.0	0.3, 0.6, 0.9, 1.2, 2.5, 3.0, 4.0
2	3	738 × 246 × 3		3.502	0.117		
3	4	984 × 246 × 3		3.565	0.107		
4	2	492 × 246 × 6	1.81	1.651	0.565		
5	3	738 × 246 × 6		1.751	0.469		
6	4	984 × 246 × 6		1.782	0.426		
7	2	492 × 246 × 7	1.55	1.415	0.769		
8	3	738 × 246 × 7		1.501	0.638		
9	4	984 × 246 × 7		1.528	0.580		

4.2.1 Impulsive pressure history shape

For single impulsive pressure loading, the effect of rising time before reaching the peak pressure P_p and the type of decay on the response of the plate was found to be negligible [30, 31]. However, this statement has not yet been confirmed for repeated impulsive pressure loadings. Therefore, in this study, to examine the effect of the profile of the triangular pressure pulse on the response of the plates, two typical profiles of impulsive pressure pulses with the same peak value were used: (1) zero rising time with linear decaying time denoted as "0tri", and (2) equal rising and decaying time denoted as "0.5tri". The considered time histories of the dynamic pressure loading, as shown in Fig. 7, were idealised as triangular pressure pulses based on the actual pressure induced by slamming. These load idealisations are characterised by two parameters, namely, the peak pressure P_p and the duration of the loading t_d.

4.2.2 Pressure magnitude and impulse duration

The peak pressure value often approaches two to three times the static collapse pressure loads P_c of the plates [32]. In this study, the upper bound solutions [19] for the static collapse pressure of fully clamped plate, were used, as shown in Eq. 3.

$$P_c = \frac{48M_p}{b^2}\frac{1}{\left(\sqrt{3+\left(\frac{b}{a}\right)^2}-\frac{b}{a}\right)^2} \tag{3}$$

where M_p is the fully plastic bending moment per unit width of the plate and is given by Eq. 4.

$$M_p = \frac{\sigma_0 \times t^2}{4} \tag{4}$$

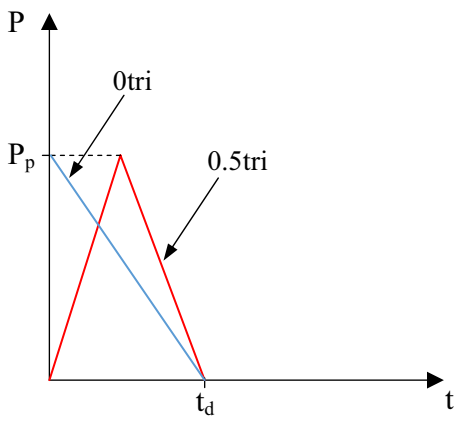

Fig. 7 Idealised slamming load profile applied for the parametric study

The selected values of P_p/P_c for the parametric study are given in Table 3. The values seem sufficiently large to result in a typical permanent set, w_p/t of the order of 1–5, without any ductile fracture in the model. In other words, only the accumulation of plastic deformations of the plates was considered in this study.

The duration of the pressure loading was considered to be in the dynamic domain and in transition between the dynamic and quasi-static domains. The normalised time parameter t_d/T_n was set in the range 0.3–4, as given in Table 3. It should be noted that T_n is the fundamental period of vibration of the plate and was determined using Eq. 5.

$$T_n = \frac{1}{f} \tag{5}$$

where f is the fundamental frequency of the plate, which was calculated using Eq. 6, unit is Hz, as proposed by Sinha [33]:

$$f = 5.544 \times 10^6 \times \frac{t}{a \times b}\sqrt{\left(\frac{a}{b}\right)^2+\left(\frac{b}{a}\right)^2+0.6045} \tag{6}$$

5 Parametric study results and discussion

The typical deformed shapes of a loaded plate shown in Fig. 8 reveal the characteristic features of the response of the plates under repeated dynamic pressure loadings. Figure 8 shows that the deformation occurs at the mid region of the plate owing to the first impact and then propagates to the boundary during the subsequent impulses; furthermore, the maximum equivalent plastic strain at integral points in thickness direction was generated at the boundaries of the plate and increased with the number of impacts. It is apparent from the figure that the permanent set of the plate increased with the number of impacts, and it tends to approach a stable state. It is observed that at the beginning, the deflection is significant, while later, it converges to a certain value, as depicted in Fig. 9. In other word, the increment in the permanent set gradually decreases when the plate is repeatedly impacted regardless of the plate aspect ratio, HAZ effect, impulse, and profile of the triangular pressure pulse. The evolution of the permanent set with the number of pressure impacts and deflection time histories were plotted to present the responses of all the plates considered in this study in the case of 10 impacts.

5.1 Effect of aspect ratio

The clamped plate was employed without considering the HAZ to investigate the effect of the aspect ratio on the permanent set evolution of the plate in the case of 10 repeated impulsive pressure loadings with the 0tri impulsive profile. The evolution of the permanent set for various plate aspect

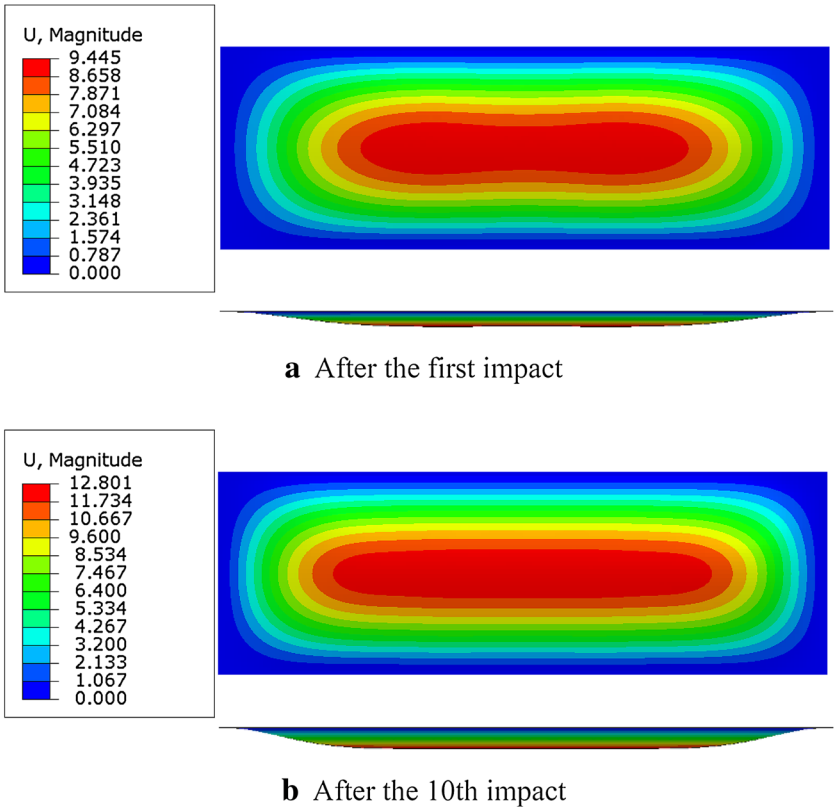

Fig. 8 Typical permanently deformed shape of the plate having *a/b* of 3 under repeated impulsive loadings with $t_d = 0.6T_n$ and $P_p = 3.0P_c$. (The contour levels represent permanent deflection)

ratios against the number of impacts is shown in Fig. 9. It can be seen from the figure that in a dynamic domain, the tendencies of the permanent set of plates throughout the 10 impacts were nearly the same, regardless of the plate aspect ratios. In other words, the increment in the permanent set was mostly the same for the various plate aspect ratios regardless of the peak pressure and load duration. In addition, the permanent set of the plate is considerably increased when the plate aspect ratio decreased, regardless of the number of impacts and impulses, as illustrated in Fig. 9.

5.2 Effect of plate slenderness ratio

The evolution of permanent set of plates, for example, having an aspect ratio of 2 for different plate slenderness ratios against the number of impacts is shown in Fig. 10. It can be seen from the figure that in dynamic domain the permanent set of plates throughout 10 impacts were increased when the plate slenderness ratio increased regardless of the plate aspect ratios, and impulses. However, it is interesting that the increment of permanent set was significantly decreased when the plate slenderness ratios increased, regardless of the peak pressure and load duration. In addition, the permanent set evolution of plate is remarkably increased when the plate slenderness ratios increased with the number of impacts, as illustrated in Fig. 10.

5.3 Effect of impulsive pressure history shape

To investigate the effect of the triangular pulse profile on the permanent set evolution of the plate in the case of 10 repeated impulsive pressure loadings, the clamped plate having an aspect ratio of 3 was employed without considering the HAZ. The normalised evolution of the permanent set for two profiles of the triangular pulse against the number of impacts is shown in Fig. 11a. As seen from the figure, when $t_d = 0.3T_n$, the permanent sets are almost the same, i.e. the permanent set of plates increases with the number of impacts, regardless of the type of triangular pulse and peak pressure. However, there are some exceptions when $P_p = 4.0P_c$ and the repetition number is greater than 5.

When $P_p = 1.5P_c$, the effects of the triangular pulse profile on the permanent set evolution of the plate were investigated changing the peak pressure values. The normalised evolution of the permanent set for two profiles of the triangular pulse against the number of impacts is shown in Fig. 11b. As seen from the figure, when t_d is $0.6T_n$, the two shapes of the impulsive pressure history provide similar deflection predictions for the first four impacts. However, from the fifth impact the monotonically decreasing impulse (0tri) shows greater permanent set than the isosceles triangular impulse (0.5tri). When t_d is $3.0T_n$, The monotonically decreasing impulse (0tri) shows greater permanent set than the other for whole impacts.

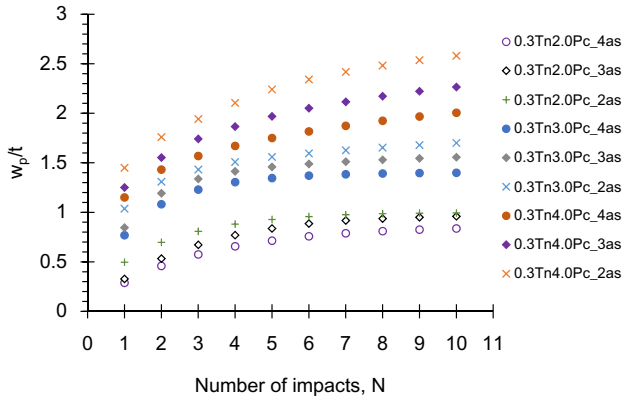

a Variation of peak pressure

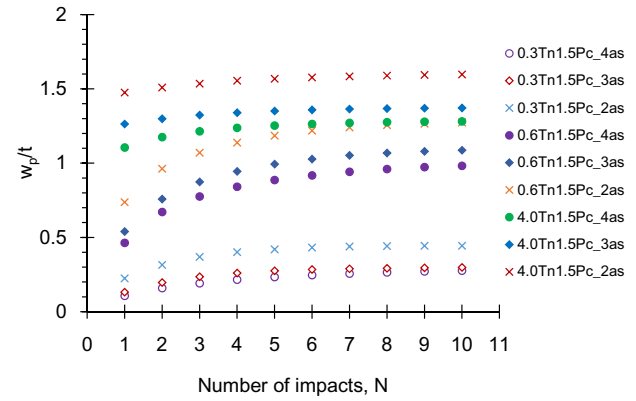

b Variation of duration

Fig. 9 Variation in normalised permanent set evolution of the plate for various cases (for example, "0.3T_n1.5P_c_4as" means that $t_d = 0.3T_n$, $P_p = 1.5P_c$, and aspect ratio $a/b = 4$)

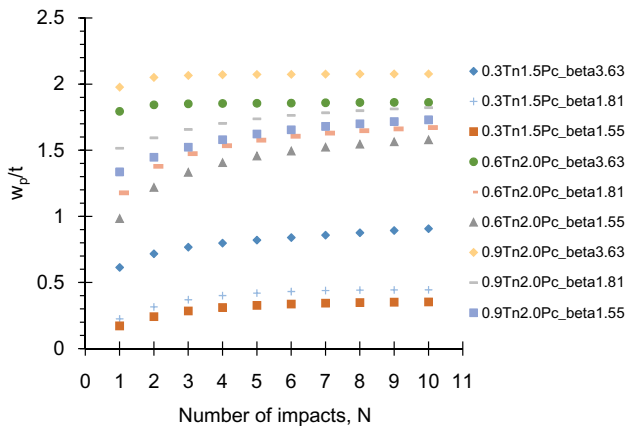

Fig. 10 Variation in normalised permanent set of plate for different plate slenderness ratio cases

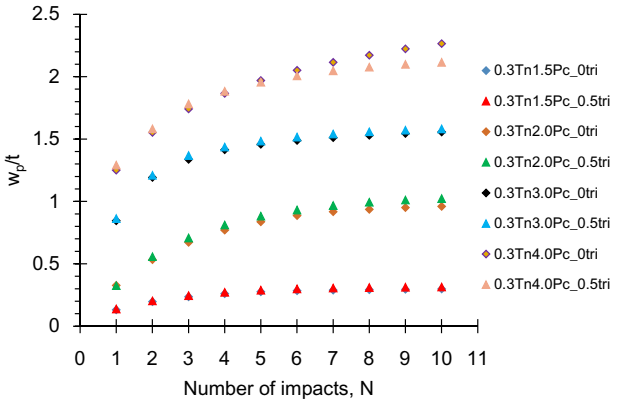

a Variation of peak pressure

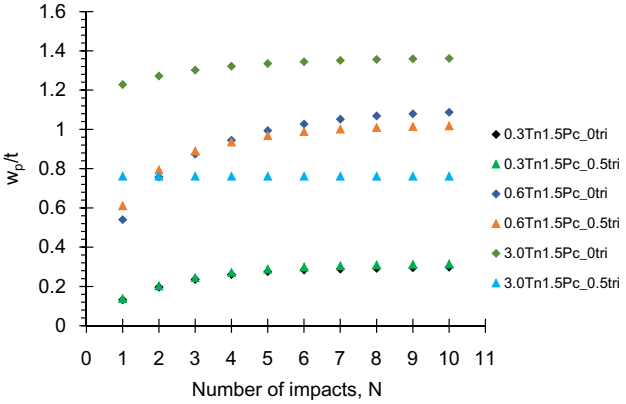

b Variation of duration

Fig. 11 Variation in normalised permanent set of plate for two different impulsive profile cases

From the practical structural design viewpoint, therefore, it can be concluded that the monotonically decreasing impulse (0tri) can be assumed to predict the permanent set evolution of plate under repeated impulsive pressure loadings induced by slamming. However, this assumption may produce over-predictions when the impulse duration is longer than the natural period, T_n.

5.4 Effect of load duration and peak pressure

The clamped plate having an aspect ratio of 3 was employed without considering the HAZ to investigate the effect of the load duration and peak pressure on the permanent set evolution of the plate in the case of 10 repeated impulsive pressure loadings with the "0tri" impulsive profile. As seen in Fig. 12, as the duration of the impact increases, there are fewer oscillations in the curves. However, even when t_d/T_n (> 3) is in the quasi-static domain, the oscillations continue to occur not only for the first impact, which was also mentioned in Ref. [34], but also for the subsequent repeated impacts. It is also observed that the increment in the permanent set of the

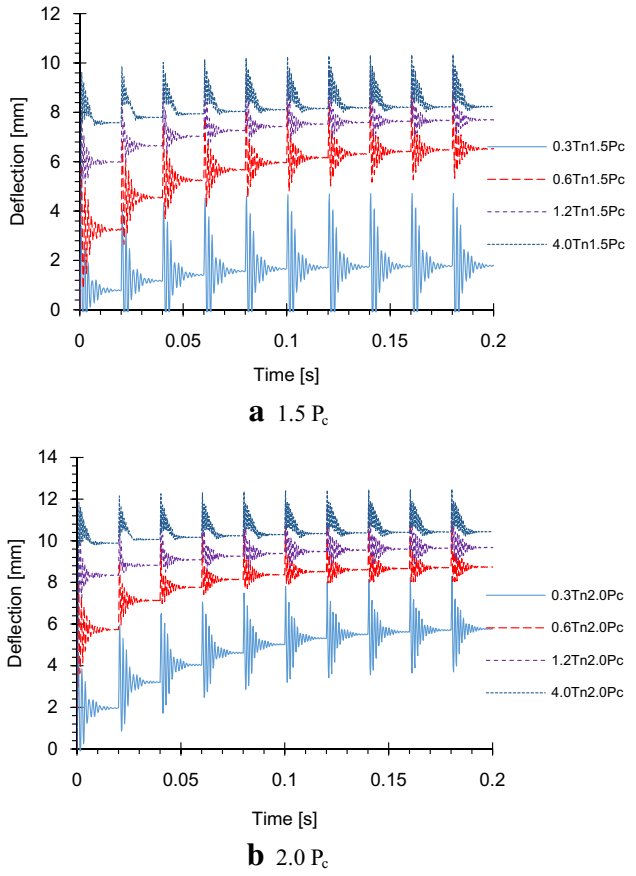

Fig. 12 Deflection time histories of plate having an aspect ratio of 3 for various cases

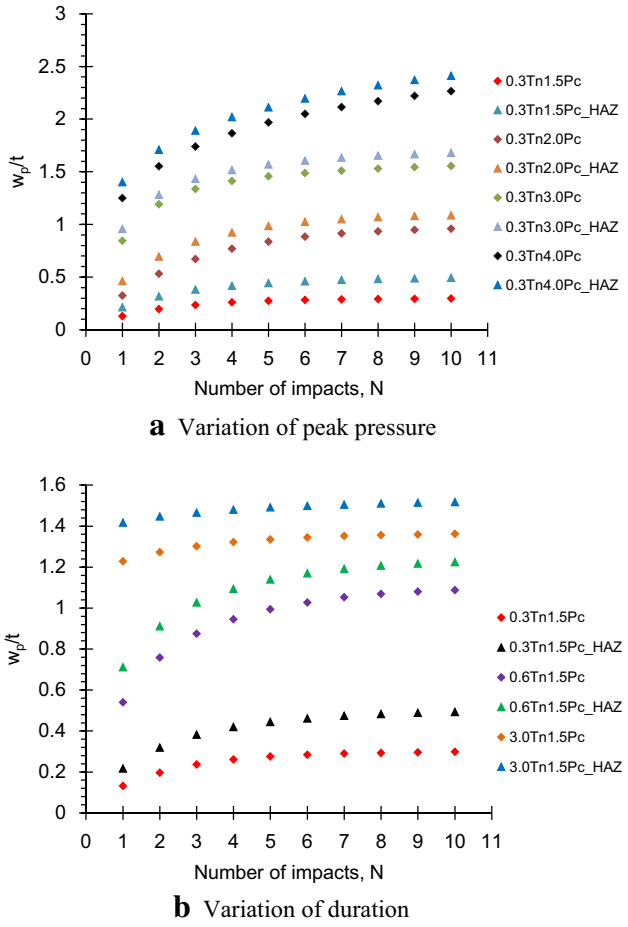

Fig. 13 Variation in normalised permanent set against number of impacts of plate having an aspect ratio of 3 with and without HAZ effects

plate is significantly decreased when higher load duration is applied. The increment in the permanent set decreases as the quasi-static domain is approached. For the case in which t_d/T_n is in the quasi-static domain, the permanent set of plate appears to remain unchanged even when the same load is applied further. However, there was a slight increase in the permanent set of the plate in the case of repeated impulses with its duration being four times the plate's natural period. Therefore, the impulse duration in the dynamic domain proposed by DNV [5] seems to be considered as longer than three times plate's natural period.

In addition, the oscillations decreased as the peak pressure P_p increased, likely due to decrease in the elastic strain energy relative to the total absorbed energy as the load magnitude increases, which was also stated by Cerik [34]. As expected, the permanent set of the plate is increased when the plate is subjected to higher impulse loadings.

5.5 Effect of heat affected zone

In addition to the effect of the impulses, the effect of the HAZ—with the assumption described in the sub-Sect. 3.4—on the extent of damage to the plate in the case of 10 repeated impulsive pressure loadings is also assessed. Here, the clamped plate having an aspect ratio of 3 and subjected to the 0tri impulsive profile was employed as a reference model. Figure 13 shows the variation of the normalised permanent set with the number of impacts of the plate, with and without the HAZ. It is evident that there is a considerable decrease in the resistance of the plate, showing increase in the permanent set of the plate impulsively loaded with HAZ, regardless of the peak pressure, load duration, and the number of impacts. However, it is observed that the increase

in the permanent set due to the HAZ decreases when the plate is impacted repeatedly. As stated in Ref. [34], considering the plastic collapse mechanism of a fully clamped rectangular plate, whereby plastic hinges are developed at the four edges of the plate, the reduced yield strength in the HAZ would be significantly affected by the response of the plates to impulsive pressure loadings. Consequently, the HAZ reduced the resistance to these loads, and less energy could thus be absorbed by the plate. It should be noted that, the increase in permanent set owing to the HAZ effects, can be associated with the assumed strength knockdown factor of 0.67. It should also be noted that this knockdown factor can vary widely depending on the type of aluminium alloys and welding methods used. It can be thus concluded that the HAZ may limit the ductile membrane deformation of the plates, and result in failure earlier than is assumed without the HAZ in this study [34].

5.6 Pseudo-shakedown phenomenon

The pseudo-shakedown phenomenon is important in marine structural design when a structure is subjected to repeated impulsive pressure loading or repeated mass impacts. Responses of marine structures under repeated impacts have been extensively investigated and discussed by experimental, theoretical and numerical methods [27, 35–39]. Regarding the repeated mass impacts, Zhu and Faulkner [36] performed repeated dynamic mass impacts on unstiffened plates and concluded that no pseudo-shakedown phenomenon occurred. The same conclusion was drawn by Cho et al. [39] when the impact energy was greater than the elastic energy absorption capacity of the beam. Huang et al. [37], by contrast, reported the achievement of the pseudo-shakedown state for plates associated with the condition of smaller kinetic energy comparing with the elastic energy absorption capacity of the plate. However, Jones [38] concluded that the external impact energy, in practice, would be greater than the elastic energy absorption capacity of the struck structure. Therefore, it would be difficult to observe the pseudo-shakedown state in reality.

Zhu et al. [40, 41] investigated the saturation phenomenon, which is a distinct feature of the dynamic response of structures subjected to a single pulse loading. This phenomenon shows that after saturation duration the rest load pulse will not cause further permanent deflection. This kind of load having a long duration can be regarded as quasi-static. It is evident that these two phenomena are related with different loading conditions. Repeated loadings are associated with the pseudo-shakedown phenomenon, whereas single loads for the saturation phenomenon, even though they are both caused by the finite-displacement effect [41]. In case of repeated impulsive pressure loadings, however, Jones [27] pointed out there was a pseudo-shakedown phenomenon for a rigid, perfectly plastic rectangular plate subjected to repeated identical slamming pressures. He observed, under certain circumstances, that a rigid, perfectly plastic structure would not deform for further repetitions of the same dynamic impulsive pressure load, i.e. when no kinetic energy can be absorbed further by the structure under repeated identical pressure pulses. A conjecture for the pseudo-shakedown phenomenon of rigid, perfectly plastic beams and plates under repeated rectangular-shaped pressure pulses has been illustrated by Shen and Jones [35].

In this study, to investigate the occurrence of the pseudo-shakedown state, numerical analyses were conducted. The analysis results of the elastic–plastic plates under various impulses are provided in Figs. 9, 10, 11 and 13. As seen in the figures, when the plate is repeatedly impacted further with (1) the same small impulse, or (2) a relatively long duration approaching quasi-static, the permanent set is getting smaller and tend towards the stationary state, which can be called as the pseudo-shakedown phenomenon, while for the repeated impact cases having short duration, but with high peak pressure, more impacts were likely required to lead to the permanent set evolution approaching a stationary value. However, it is still premature to figure out when the plate reaches its pseudo-shakedown state. Further experimental and numerical investigations seem necessary to draw any firm conclusion regarding the occurrence of the pseudo-shakedown state.

According to the case study of repeated impacts, it can be concluded that the peak pressure and duration and number of impact, as well as the material properties have a significant effect on whether the pseudo-shakedown state can be achieved for a structure under repeated impulsive pressure loadings. It should be noted that the present study only refers to the plastic deformation mode, while the fracture damage mode have not been considered, which in practice could cause no achievement of a pseudo-shakedown state.

6 Design equations for predicting permanent set evolution

For a more deliberate design of marine structures, it is necessary to be able to estimate the damage evolution of plates under the repeated impulsive pressure loadings induced by

Fig. 14 Tendencies of permanent set of plates (without HAZ) with non-dimensional design parameters

slamming. In the available literature, there are many studies focusing on the estimation of a permanent set of the plates due to a single impulse; however, during the service life of marine structures, the single impulse may not be a likely representation of realistic slam loads acting on structures. However, there exists no formulation for predicting the permanent set evolution of structures caused by repeated impulsive pressure loadings.

It was, therefore, decided to derive a design formulation for predicting the evolution of the permanent set of the plates subjected to repeated monotonically decreasing triangular impulses. Prior to deriving the design formulae, the tendencies of non-dimensional design parameters were investigated, based on the results of rigorous parametric studies performed, as shown in Figs. 9, 10, 11, 13 and 14. The non-dimensional parameters, such as the aspect ratio (a/b), plate slenderness ratio (β), peak pressure (P_p/P_c), peak duration (t_d/T_n), and impact numbers (N), are used. As can be observed in the figures, the evolution of the permanent set is monotonically increased according to the non-dimensional design parameters, except the peak duration, plate slenderness ratio and the number of impacts. When the peak durations, plate slenderness ratio and impact numbers increased, the permanent set tended to have certain values. The form of the equation for the prediction of the permanent set can be then selected. As observed by Cho et al. [28], Eq. 7 is the basis for providing a good fit for the variation of the permanent set with t_d/T_n, β and N. In addition, the other two parameters (P_p/P_c and a/b) can be considered as modification factors for this equation. It should be noted that this form was also reliably applied by Cerik [34] in deriving equations for predicting the permanent set of the plates due to a single pulse.

$$f(x) = \frac{x}{\sqrt{1+x^2}} \tag{7}$$

By performing a nonlinear regression analysis, Eqs. 8 and 9, are derived for predicting the permanent set evolution of the plates without and with the HAZ effect, respectively, under repeated impulsive pressure loadings induced by slamming, as functions of the peak pressure, peak duration of the impulse, number of impacts, and plate slenderness and aspect ratios. It should be noted that only the dynamic domain ($0.3 < t_d/T_n < 3$) with P_p/P_c in a range 1.5–4.0 is applied to plate, is considered in deriving the following equations:

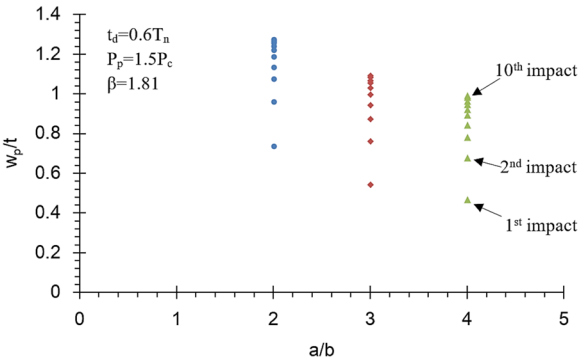

a Aspect ratio

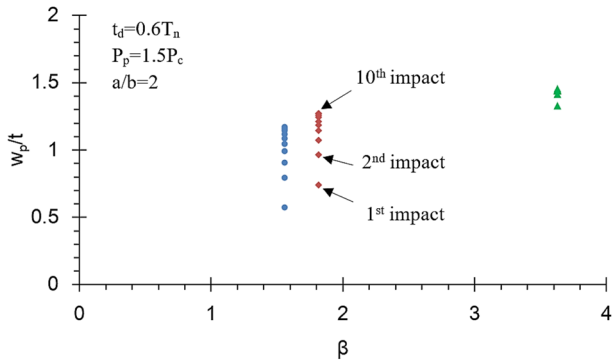

b Slenderness ratio

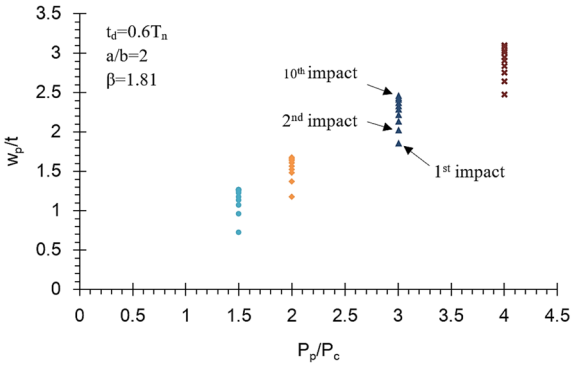

c Peak pressure

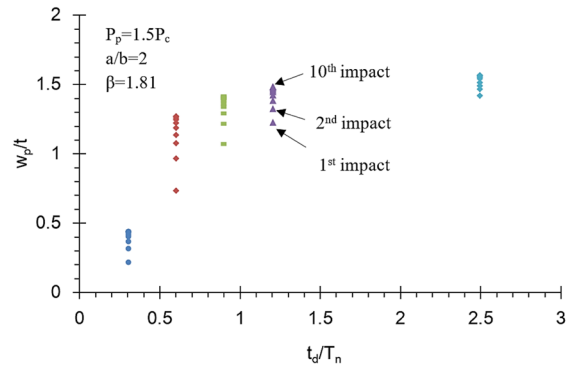

d Peak duration

For a plate without the HAZ:

$$\frac{w_p}{t} = 1.62\left[\left(\frac{N}{\sqrt{1+0.01N^2}}\right)^{0.06}\left(\frac{T_p/T_n}{\sqrt{1+(T_p/T_n)^2}}\right)^{0.35} \times \left(\frac{\beta}{\sqrt{1+\beta^2}}\right)^{2.26}\left(\frac{P_p}{P_c}\right)^{0.96}\left(\frac{a}{b}\right)^{-0.37}\right] \quad (8)$$

with a mean of 0.998 and coefficient of variation (COV) of 6.41%.

For a plate with the HAZ

$$\frac{w_p}{t} = 2.05\left[\left(\frac{N}{\sqrt{1+0.01N^2}}\right)^{0.04}\left(\frac{T_p/T_n}{\sqrt{1+(T_p/T_n)^2}}\right)^{0.35} \times\left(\frac{\beta}{\sqrt{1+\beta^2}}\right)^{2.73}\left(\frac{P_p}{P_c}\right)^{0.87}\left(\frac{a}{b}\right)^{-0.35}\right] \quad (9)$$

with a mean of 1.008 and COV of 5.56%.

For all the equations, the ratio of the predicted w_p/t using the above equations to the numerical analysis results is calculated. After deriving any design formulation, it is necessary to check the skewness of the predictions against numerical results using the cross-validation charts, as shown in Fig. 15. The accuracy and reliability of the predictions using the proposed design formulation are acceptable. It should be noted that for all the equations, there is a slight discrepancy when t_d/T_n is less than 0.6 for the first impact and less than 0.5 for all the subsequent impacts.

7 Conclusions

In this study, the results of the repeated wet drop tests conducted on stiffened plates by Mori [9] were used to provide information for the validation of the current FE analysis model of the plates under repeated impulsive loadings. The response of marine aluminium-alloy rectangular plates to repeated impulsive pressure loads was then numerically studied. The material characteristics and the HAZ were also taken into account. The validation model was then used for a rigorous parametric study to evaluate the effect of a number of key parameters such as the peak pressure, impact duration and aspect and slenderness ratios on the response of the aluminium plates. Nonlinear regression analysis was then performed and design formulae were presented. The findings of this study are as follows:

When the wet drop tests are repeatedly performed for the same drop height, the increases in the permanent set of the impacted plate cannot be neglected. However, when the same quasi-static load is applied several times, the permanent set does not be increased.

The numerical analysis results of the repeated impulsive pressure impacts show that in the beginning, the increases in the permanent set are significant, but later, the total

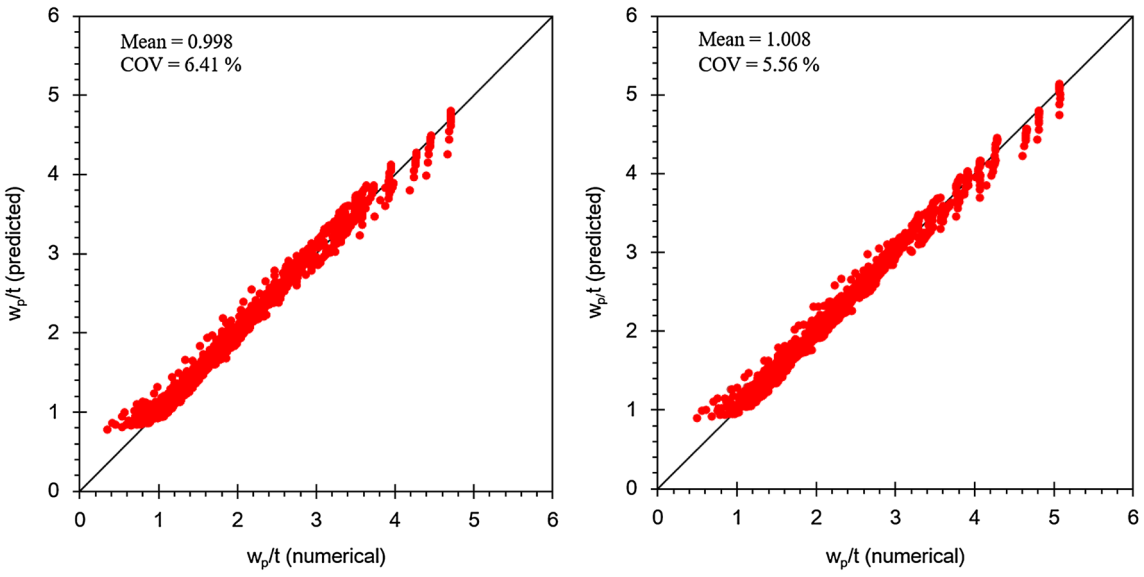

a Neglecting HAZ **b** Considering HAZ

Fig. 15 Comparison of the predicted damage evolution of the plates using the proposed formulas with the numerically observed data in the dynamic domain

permanent set converges to a certain value, regardless of the plate aspect ratio, HAZ effect, impulse, or profile of the triangular pressure pulse.

In a dynamic domain, the permanent set of the plates at the first three impacts was almost identical regardless of the plate aspect ratio, whereas they were clearly different to each other in the quasi-static domain. However, the increment in the permanent set was mostly the same for different plate aspect ratios, regardless of the peak pressure and load duration. In addition, the permanent set of the plate is considerably increased when the plate aspect ratio is decreased and the plate slenderness ratio is increased, regardless of the number of impacts and impulses.

For a single impulsive load, the response of the plate is not significantly affected by the profile of the triangular pressure pulse, whereas in the case of repeated impulsive pressure loadings that are often induced by actual slamming during the service life of vessels, the shape of the pressure time history considerably affects the response of the plates. Therefore, the realistic pressure time history arising from slamming should be carefully considered in the structural design of high-speed vessels.

Reported experimental investigations and theoretical analyses have been briefly reviewed and the numerical analyses of repeated impact problem were developed in this study. A brief discussion on the pseudo-shakedown phenomenon was provided. The impulse characteristics, number of impacts, and material properties were highlighted as important parameters in the structural response under repeated impacts.

Using the results obtained through extensive numerical simulations, simple yet accurate design formulae for prediction of the permanent set of plates under repeated impulsive pressure loadings induced by slamming were derived as a function of non-dimensional impulse parameters, plate slenderness and aspect ratios, and the number of impacts. The simple formulae proposed are in good agreement with the numerical analysis results.

The effect of the HAZ on the boundaries of the plates was found to be significant. It is evident that there is a considerable decrease in the resistance of the plate, which indicates an increase in the permanent set of the plate that is impulsively loaded when considering HAZ, regardless of the impulses and the number of impacts. However, it is observed that the increase in the permanent set due to the HAZ decreases when the plate is impacted repeatedly.

The results of this study can be applied to the structural design of high-speed vessels subjected to repeated impulsive pressure loadings induced by slamming. Till date, experiments focusing on aluminium-alloy panels subjected to repeated impulsive pressure loadings have rarely been conducted. Hence, further experimental test results for the impact response of marine aluminium-alloy plates are desirably required considering the typical slamming load in addition to the properties of the HAZ formed due to the fusion welding process. Moreover, further investigation appears to be necessary with respect to the effects of the strain hardening and strain-rate hardening on the dynamic response of marine aluminium-alloy plates to repeated impulsive pressure loadings.

Acknowledgements This work was supported by the Korea Institute of Energy Technology Evaluation and Planning (KETEP) and the Ministry of Trade, Industry and Energy (MOTIE) of the Republic of Korea (No. 20154030200970).

References

1. DNV (2016) Rules for high-speed, light craft and naval surface craft, P.3, Ch.1, July
2. ABS (2013) Rules for building and classing high-speed craft, Pt. 3 Ch.2, pp 57
3. GL (2012) Rules and guidelines, I-Pt.3, Ch.1, pp 3-17
4. Greenspon JE (1956) Sea tests of the USCGC Unimak, Part 3—Pressures, strains and deflections of the bottom plating incident to slamming. DTMB Report;978
5. DNV (2010) Design against accidental loads. Recommended practice, DNV-RP-C204. Det Norske Veritas, Høvik, Norway
6. Yuhara T (1975) Fundamental study of wave impact loads on ship bow (3rd report). J Soc Naval Archit Jpn 137:240–245
7. Caridis P, Stefanou M (1997) Dynamic elastic/viscoplastic response of hull plating subjected to hydrodynamic wave impact. J Ship Res 41(2):130–146
8. Shin HK, Lee DW, Park J, Cho S-R (2016) Damage of plates due to repeated impulsive pressure loadings. In: Proceedings of 13th international symposium on practical design of ships and other floating structures (PRADS 2016), Copenhagen, Denmark
9. Mori K (1977) Response of the bottom plate of high-speed crafts under impulsive water pressure. J Soc Naval Archit Jpn 142:297–305 **(in Japanese)**
10. Mori K, Nagai T (1976) Response of stiffened plates under impulsive water pressure. J Soc Naval Archit Jpn 140:165–173 **(in Japanese)**
11. Kristensen OHH (2001) Ultimate capacity of aluminium plates under multiple loads considering HAZ properties, Ph.D thesis, Norwegian University of Science and Technology
12. Paik JK, Duran A (2004) Ultimate strength of aluminum plates and stiffened panels for marine structures. Mar Technol 41(3):108–121
13. Paik JK, Andrieu C, Cojeen HP (2007) Mechanical collapse testing on aluminum stiffened plate structures for marine applications. In: Proceedings of 10th International symposium on practical design of ships and other floating structures (PRADS 2007), Houston
14. Benson S, Downes J, Dow RS (2013) A comparison of numerical methods to predict the progressive collapse of lightweight aluminium vessels. J Ship Prod Des 29(3):117–126
15. Villavicencio R, Guedes Soares C (2011) Numerical modeling of the boundary conditions on beams struck transversely by a mass. Int J Impact Eng 38(5):384–396
16. Park BW, Cho S-R (2006) Simple design formulae for predicting the residual damage of unstiffened and stiffened plates under explosive loadings. Int J Impact Eng 32:1721–1736

17. Minamoto H, Seifried R, Eberhard P, Kawamura S (2011) Analysis of repeated impacts on a steel rod with visco-plastic material behavior. Eur J Mech A/Solids 30:336–344
18. Henchie TF, Chung Kim Yuen S, Nurick GN, Ranwaha N, Balden VH (2014) The response of circular plates to repeated uniform blast loads: an experimental and numerical study. Int J Impact Eng 74:36–45
19. Jones N (1989) Structural impact, 1st edn. Cambridge University Press, Cambridge
20. Park DH, Choi SW, Kim JH, Lee JM (2015) Cryogenic mechanical behavior of 5000 and 6000 series aluminium alloys: issues on application to offshore plants. Cryogenics 68:44–58
21. Benson S, Downes J, Dow RS (2013) Load shortening characteristics of marine grade aluminium alloy plates in longitudinal compression. Thin Wall Struct 70:19–32
22. Zha Y, Moan T (2001) Ultimate strength of stiffened aluminium panels with predominantly torsional failure modes. Thin Wall Struct 39(8):631–648
23. Rigo P, Sarghiuta R, Estefen S, Lehmann E, Otelea SC, Pasqualino I, Simonsen BC, Wan Z, Yao T (2003) Sensitivity analysis on ultimate strength of aluminium stiffened panels. Mar Struct 16:437–468
24. Khedmati MR, Zareei MR, Rigo P (2009) Sensitivity analysis on the elastic buckling and ultimate strength of continuous stiffened aluminium plates under combined in-plane compression and lateral pressure. Thin Wall Struct 47:1232–1245
25. Khedmati MR, Pedram M (2014) A numerical investigation into the effects of slamming impulsive loads on the elastic–plastic response of imperfect stiffened aluminium plates. Thin Wall Struct 76:118–144
26. Paik JK, Thayamballi AK, Ryu JY, Jang JH, Seo JK, Park SW, Soe SK, Renaud C, Kim NI (2008) Mechanical collapse testing on aluminum stiffened panels for marine applications. Ship Structure Committee Report, SSC-451, pp 1232–1245
27. Jones N (1973) Slamming damage. J Ship Res 17(2):80–86
28. Cho S-R, Lim W-R, Park C-B (2011) Development of design formula for predicting damage extents of unstiffened plates under impulsive pressure loadings. In: Proceedings of 25th Asian-Pacific technical exchange and advisory meeting on marine structures (TEAM 2011). Incheon, Korea, pp 699–706
29. ABAQUS User's Manual Version 6.10 (2010)
30. Paik JK, Lee JM, Shin YS, Wang G (2004) Design principles and criteria for ship structures under impact pressure actions arising from sloshing, slamming and green water. Trans SNAME 112:292–313
31. Cho S-R, Elangovan M, Engle A, Ha T, Jensen JJ, Kapsenberg G, Malenica S, Matagne J, Ren H, Rosen A, Saevik S, Temarel P, Uhlenbrock S, Yoshikawa T (2012) Report of committee V.7: impulse pressure loading and response assessment. In: Proceedings of 18th international ship and offshore structures congress (ISSC2012);2, Rostock, Germany, pp 205–329
32. Paik JK (2006) Toward limit state design of ships and offshore structures under impact pressure actions: a state-of-the-art-review. Mar Technol 43(3):135–145
33. Sinha S, Kar S, Sarangdhar DG (2008) Development of simplified structural design formulation for slamming loads. In: Proceedings of the ASME 27th International Conference on Ocean, Offshore and Arctic Engineering, OMAE2008-57740, Estoril
34. Cerik BC (2017) Large inelastic deformation of aluminium alloy plates in high-speed vessels subjected to slamming. J Mar Sci Technol 22(2):301–312
35. Shen WQ, Jones N (1992) The pseudo-shakedown of beams and plates when subjected to repeated dynamic loads. J Appl Mech 59(1):168–175
36. Zhu L, Faulkner D (1996) Damage estimate for plating of ships and platforms under repeated impacts. Mar Struct 9:697–720
37. Huang ZQ, Chen QS, Zhang WT (2000) Pseudo-Shakedown in the collision mechanics of ships. Int J Impact Eng 24:19–31
38. Jones N (2014) Pseudo-shakedown phenomenon for the mass impact loading of plating. Int J Impact Eng 65:33–39
39. Cho S-R, Truong DD, Shin HK (2014) Repeated lateral impacts on steel beams at room and sub-zero temperatures. Int J Impact Eng 72:75–84
40. Zhu L, Yu TX (1997) Saturated impulse for pulse-loaded elastic-plastic square plates. Int J of Sol Struct 34(14):1709–1718
41. Zhu L, Bai X, Yu TX (2017) The saturated impulse of fully clamped square plates subjected to linearly decaying pressure pulse. Int J Impact Eng (In press). https://doi.org/10.1016/j.ijimpeng.2016.12.012